# Influence of temperature on the frictional properties of water-lubricated surfaces

**Lee, Seunghwan; Røn, Troels**

*Published in:*
Lubricants

*Link to article, DOI:*
10.3390/lubricants2040177

*Publication date:*
2014

*Document Version*
Publisher's PDF, also known as Version of record

*Lubricants* **2014**, *2*, 177-192; doi:10.3390/lubricants2040177

OPEN ACCESS

*lubricants*

**ISSN 2075-4442**

www.mdpi.com/journal/lubricants

*Article*

# Influence of Temperature on the Frictional Properties of Water-Lubricated Surfaces

**Troels Røn and Seunghwan Lee ***

Department of Mechanical Engineering, Technical University of Denmark, Kgs. Lyngby DK-2800, Denmark; E-Mail: tror@mek.dtu.dk

* Author to whom correspondence should be addressed; E-Mail: seele@mek.dtu.dk; Tel.: +45-4525-2193; Fax: +45-4525-6213.

External Editor: Hong Liang

*Received: 10 July 2014; in revised form: 12 August 2014 / Accepted: 10 September 2014 / Published: 15 October 2014*

---

**Abstract:** The influence of temperature on the lubricating properties of neat water for tribopairs with varying bulk elasticity moduli and surface hydrophilicity, namely hard-hydrophobic interface (*h*-**HB**), hard-hydrophilic interface (*h*-**HL**), soft-hydrophobic interface (*s*-**HB**), and soft-hydrophilic interface (*s*-**HL**), has been investigated. With increasing temperature, the coefficients of friction generally increased due to the decreasing viscosity of water. This change was more clearly manifested from soft interfaces for more feasible formation of lubricating films. Nevertheless, dominant lubrication mechanism appears to be boundary and mixed lubrication even for soft interfaces at all speeds (up to 1200 mm/s) and temperatures (1 to 90 °C) investigated. The results from this study are expected to provide a reference to explore the temperature-dependent tribological behavior of more complex aqueous lubricants, e.g., those involving various additives, for a variety of tribosystems.

**Keywords:** aqueous lubrication; temperature; soft; hard; hydrophilic; hydrophobic

---

## 1. Introduction

Biomimetics has been drawing increasing attention in modern science and technology as various interesting and useful inspirations can be acquired from biological systems in order to solve the

problems in engineering systems. Lubrication is not an exception; extensive efforts to utilize the principles of biological lubrication for man-made, engineering tribosystems have been put forth in the past a couple of decades [1–3]. One of the instrumental approaches in this endeavor is to use water as base lubricant [1–5], mimicking, for example, life-long maintenance of synovial joints of human and animals [6,7]. Industrial application of water-based lubricants is desirable from economic and environmental standpoints as well since water is abundant, non-toxic, and an effective coolant. Moreover, water is practically the only viable base stock in biomedical applications due to the requirement of biocompatibility.

Beyond biomedical engineering, however, practical use of water as base lubricant is presently limited [8,9]. This is mainly due to that viscosity, and more importantly pressure coefficient of viscosity of water, is too low, resulting in, even at relatively high entrainment speeds, insufficient fluid film formation, which hampers activation of elastohydrodynamic lubrication (EHL) [10,11]. In order to broaden the scope of industrial applications of aqueous lubrication, several subjects must be further understood. One of them is the influence of temperature. Most bearing systems operate at higher temperatures than room temperature. While a number of previous studies have investigated the lubricating properties of water for various materials, absolute majority of them were studied at room temperature [4,10–13], whereas those at other temperatures than ambient are rare to date [14]. At elevated temperatures, many parameters affecting aqueous lubrication may change. Most apparently, the viscosity of base lubricant, water, would be decreasing with increasing temperature. Generally, the relationship between temperature and viscosity of organic liquids is expressed similarly with chemical reactions, such as:

$$\eta = \eta_0 \cdot e^{\frac{\Delta E_a}{kT}} \tag{1}$$

where $\eta$ and $\eta_0$ are viscosities at elevated and ambient temperatures [15,16]. The influence of temperature on the viscosity of water is empirically well established, and also shows exponentially decreasing trend with increasing temperature: from 1.793 mPa·s to 0.282 mPa·s from 0 °C to 100 °C [17]. A general expectation of reduced viscosity of lubricants in fluid-film lubrication is decreasing film thickness with increasing temperature [18,19]. However, its influence in boundary or mixed lubrication regimes, in which aqueous lubrication typically occurs, is much more complex, since it is dependent on various surface properties of interacting tribopairs [20–22]. As aqueous lubricants can include a variety of additives, which may exhibit additional complexity in response to temperature change, it is important to establish the impact of temperature on the lubricating properties of base lubricant, neat water, first.

In this context, we have investigated the lubricating properties of neat water for various tribological contacts with varying temperature, therefore, to formulate a reference for further complex aqueous lubricant systems involving a variety of additives. Since the efficacy of water-based lubrication is known to be greatly influenced by bulk elasticity moduli [20,21], as well as surface hydrophilicity [22] of tribopairs, these two parameters have been systematically varied, and four tribopairs have been employed: hard-hydrophobic interface (*h*-**HB**, self-mated polyoxymethylene (POM)), hard-hydrophilic interface (*h*-**HL**, steel-glass), soft-hydrophobic interface (*s*-**HB**, self-mated poly(dimethylsiloxane (PDMS)), and soft-hydrophilic interface (*s*-**HL**, self-mated oxidized PDMS).

## 2. Results and Discussion

### *2.1. Theoretically Predicted Lubricating Properties: Lubricating Film Thickness*

A numerical model proposed by Hamrock and Dowson [20], which was later revised by Esfahanian and Hamrock [21], provides a useful first guideline to estimate the lubricant film thickness as a function of materials parameters, including tribopairs' elasticity moduli and lubricant's viscosity, as well as operating parameters, such as load and entrainment speed. In order to identify the EHL regime to which the tribological contacts in this study belong, *i.e.*, among isoviscous-rigid (IR), piezoviscous-rigid (VR), isoviscous-elastic (IE), and piezoviscous-elastic (VE) regimes, dimensionless viscosity parameter, $g_E$, and dimensionless elasticity parameter, $g_V$, must be evaluated first [20,21]. It was confirmed that all the tribological contacts under the experimental conditions in this study belong to isoviscous-elastic (IE) regime (or as known as "soft EHL" regime). The results of the calculations are shown in Supplementary Data (SD1). Then, the minimum lubricating film thickness ("lubricating film thickness", hereafter) for circular contacts can be estimated according to the equation:

$$h = 3.28\left(w^{-0.21}E'^{-0.45}\eta_0^{0.66}u^{0.66}R_x^{0.76}\right) \quad (2)$$

where $\eta_0$ is lubricant's viscosity at atmospheric pressure, $u$ is mean speed, $E'$ is reduced Young's modulus, $w$ is applied load, $R_x$ is radius in the $x$ direction, which is equal to $R_y$ in circular contact. It is noted that pressure viscosity coefficient is not included as a parameter to influence the lubricating film thickness in soft EHL regime.

The calculated film thicknesses according to the Hamrock and Dowson Equation (1) are presented in Figure 1 for (a) POM-POM; (b) steel-glass; and (c) PDMS-PDMS.

**Figure 1.** Plots of minimum film thickness ($h$) as a function of speed, (**a**) $h$-**HB** interface (POM-POM); (**b**) $h$-**HL** interface (steel-glass); and (**c**) $s$-**HB** and $s$-**HL** interfaces (PDMS-PDMS and *ox*PDMS-*ox*PDMS).

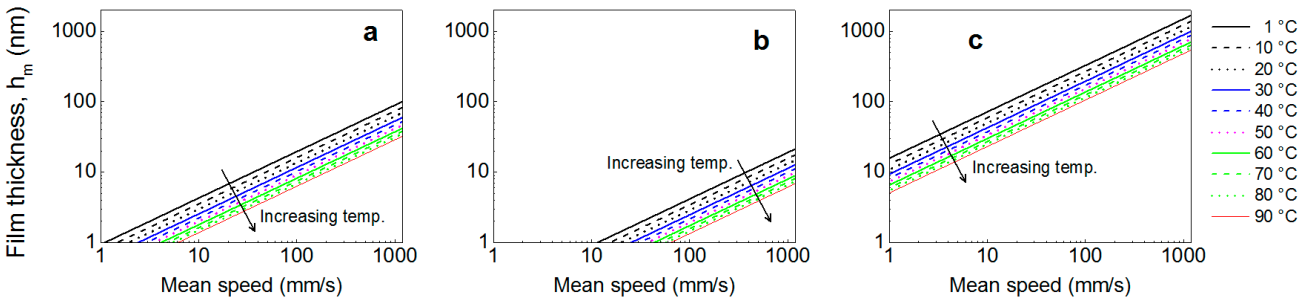


For all cases, the lubricating film thickness was expected to be increasing with increasing speed. The expected film thickness was in the order of PDMS-PDMS > POM-POM > steel-glass at all temperatures. Temperature is not included as an explicit parameter affecting the thickness of lubricating film in Equation (2), but has, in fact, a significant influence as the viscosity of lubricant (water), $\eta_0$, is expected to change with varying temperature. The change of elasticity moduli of hard materials ($E'$) in this study, e.g., glass, steel, POM, within 1–90 °C is not expected [23,24]. Corresponding change for PDMS is un-ignorable [25], but its ultimate influence on the calculated film

thickness is of little significance; for instance, the decrease of lubricating film thickness solely due to the increase of elasticity modulus of PDMS at the highest temperature, 90 °C, compared to that at 1 °C is expected to be only 12%. Further details on the calculations are provided in SD2 in Supplementary Data.

### *2.2. Theoretically Predicted Lubricating Properties: Consideration of Surface Properties*

The estimation of lubricating film thickness according to Equation (1), however, does not take into account surface parameters such as surface roughness and surface hydrophilicity of the tribopairs. Among them, the influence of surface roughness on the lubrication regime can be readily quantified by obtaining Stribeck parameter or lambda (λ) parameter: λ = (film thickness)/(root-mean-square roughness), where λ parameter is defined as $\lambda = h/(\sigma_{ball}^2 + \sigma_{disc}^2)^{½}$, where $\sigma_x$ are the root-mean-square roughness of ball and disc substrates. The calculated λ parameters are in the order of POM-POM < steel-glass < PDMS-PDMS as a function of speed (not shown). λ parameters were plotted as a function of temperature in Figure 2 from 1 °C to 90 °C by the increment of 10 °C at 10, 100, and 1000 mm/s: (a) POM-POM; (b) steel-glass; and (c) PDMS-PDMS tribopairs.

**Figure 2.** Plots of lambda parameter (λ) *vs.* as a function of temperature for the three tribopairs: (**a**) *h*-**HB** interface (POM-POM); (**b**) *h*-**HL** interface (steel-glass); and (**c**) *s*-**HB** and *s*-**HL** interfaces (PDMS-PDMS and *ox*PDMS-*ox*PDMS).

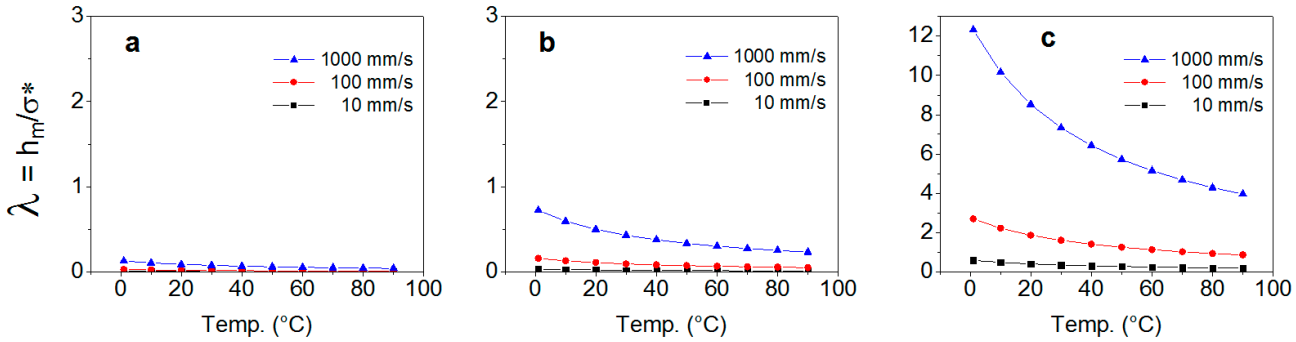


For all tribopairs, λ parameters were estimated to be decreasing with increasing temperature, as a result of decreasing viscosity, *i.e.*, $h \propto \eta_0^{0.66}$. According to a conventional view, λ has to be 3 or higher for full-fluid lubricating films to be formulated [26,27]. However, the threshold λ value for the activation of fluid-film has been reported to be highly variant, and somewhat larger values are proposed for deformable surfaces as elastomers [28,29]. Nevertheless, it is clear that both hard tribopairs showed extremely low λ values; for example, λ ≈ 0.25 even at 1 °C for steel-glass pair, where the film thickness should be highest. Thus, elastohydrodynamic lubrication is hardly expected at any temperature. Due to very high surface roughness of POM ball and disc (see Table 1), the λ parameters of POM-POM pair were calculated to be lowest at all conditions. For PDMS-PDMS pair, as well as *ox*PDMS-*ox*PDMS pair, PDMS disc was extremely smooth on surface, but PDMS ball showed fairly high surface roughness, replicating the surface roughness of the aluminum mold (Table 1). Thus, in high-speed regime (1000 mm/s), λ parameter of *ca.* 12 to 4 is expected from 1 to 90 °C. But in the medium- (100 mm/s) and low-speed (10 mm/s) regimes, λ parameters were estimated to be lower than 3 at all temperatures.

### *2.3. Experimentally Determined Friction Forces*

Lubricating film thickness can be experimentally determined by means of interferometry [30–32]. However, this technique is applicable to a limited range of materials as tribopair, and cannot cover all the materials in this study. Thus, the experimental assessment of the predicted lubricating film thickness was carried out by measuring and comparing with coefficients of friction, as will be shown below in detail. Since the relationship between lubricating film thickness and friction forces is non-trivial, it should be noted that friction forces cannot be a direct probe of the lubricating film thickness. The influence of temperature on the frictional properties of the four tribopairs lubricated with water was investigated by acquiring $\mu$ *vs.* mean speed with MTM, and plotting $\mu$ *vs.* Sommerfeld number (speed × viscosity × load$^{-1}$) as a function of temperature.

#### 2.3.1. Hard Interfaces

As shown in Figure 3, for *h*-**HB** interface, the $\mu$ values were very weakly dependent on the speed, and only a slight decreasing trend of $\mu$ was observed with increasing speed at all temperatures.

**Figure 3.** (**a**) $\mu$ *vs.* mean speed (**b**) $\mu$ *vs.* Sommerfeld number (mean speed × viscosity × load$^{-1}$) plots for *h*-**HB** interface (POM-POM) lubricated with water as characterized by MTM. All experiments were performed in water at 50% SRR. Temperature was increased from low (1 °C) to high (90 °C). Each point in the plots consists of averaging three measurements. Error bars designate standard deviation from the average values.

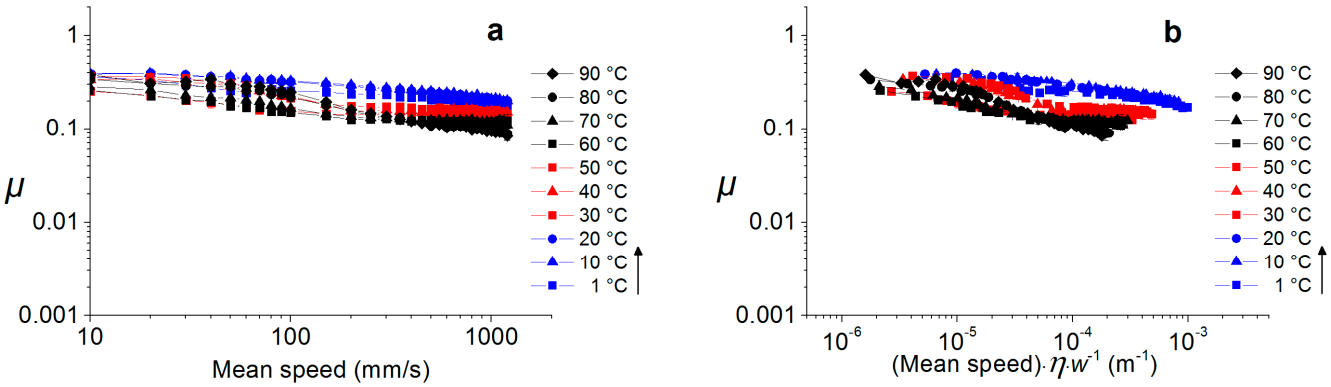


The $\mu$ values remained within 0.1–0.4 over the entire range of speed at all temperatures. The conversion of the $\mu$ *vs.* speed plots to $\mu$ *vs.* Sommerfeld number plots (Figure 3b) did not change somewhat scattered data points, and in fact, they appear to scatter slightly more by the conversion. This is closely related to the fact that POM surface is hydrophobic, hard, and rough, thus, resulting in harsh asperity contacts. Consequently, water is mostly expelled from the interface. In fact, the $\mu$ *vs.* speed plots obtained from dry sliding contacts of POM-POM at 20 °C (data not shown) were not distinguishable from those obtained in water. Thus, POM-POM sliding in water has essentially the characteristics of dry sliding contact, and insignificant changes of $\mu$ over the entire range of temperature are also resulted from it even in water. A previous study has also reported stable and consistent $\mu$ values from the self-mated contact of POM in air up to *ca.* 150 °C [14].

Figure 4 shows $\mu$ *vs.* speed plots and $\mu$ *vs.* Sommerfeld number plots for *h*-**HL** interface (steel *vs.* glass) at various temperatures.

**Figure 4.** (**a**) $\mu$ *vs.* mean speed (**b**) $\mu$ *vs.* Sommerfeld number (mean speed × viscosity × load$^{-1}$) plots for *h*-**HL** interface (steel-glass) lubricated with water as characterized by MTM. All experiments were performed at 50% SRR. Temperature was increased from low (1 °C) to high (90 °C). Each point in the plots consists of averaging of three measurements. Error bars designate standard deviation.

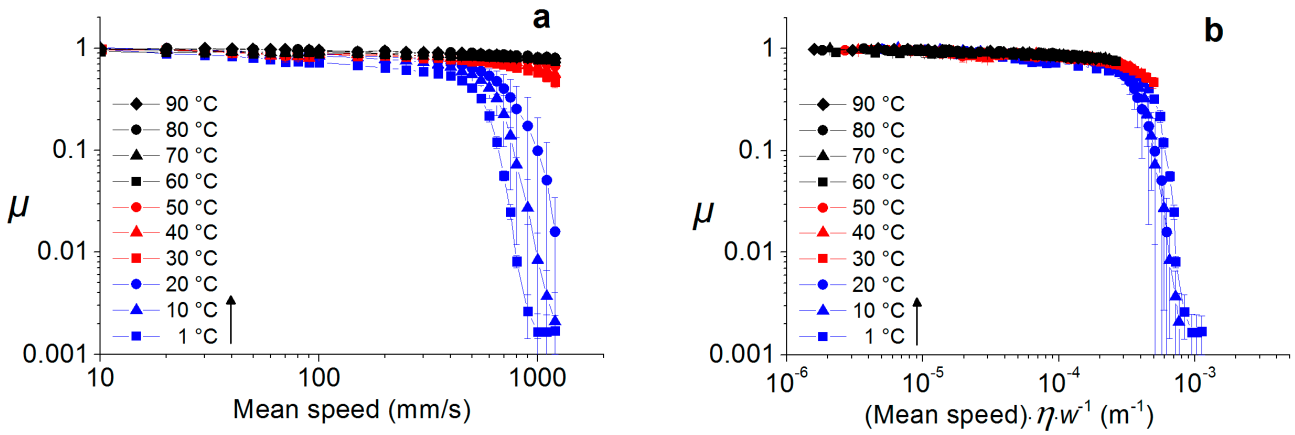


Although much higher $\mu$ values compared to *h*-**HB** pair were observed in low- and medium-speed regimes (10–100 mm/s), $\mu$ being close to 1, a rapid decrease in $\mu$ values with increasing speed was observed at low temperatures (20 °C or lower). Based on the elasticity moduli, it is expected to be more difficult for steel-glass pair to form lubricating film than POM-POM interface (Figure 1b). By taking the surface roughness into account, however, λ parameters of the former are slightly higher than those of the latter (Figure 2b). Nevertheless, λ parameters of both hard tribopairs are very small (maximum *ca.* 0.72 for steel-glass and *ca.* 0.13 for POM-POM at 1 °C, 1000 mm/s) that the difference in λ parameters cannot solely account for a large difference in $\mu$ values in high-speed regime. This lubricating effect is attributed to superior water wettability of the steel-glass tribopair compared to POM-POM. The conversion of the $\mu$ *vs.* speed plots to the $\mu$ *vs.* Sommerfeld number (Figure 4b) plots has revealed an overlap of the data points on a master curve. With increase of Sommerfeld number, activation of mixed lubrication is apparent.

Overall, the influence of temperature on the lubrication with water is generally weak for both hard interfaces. This is firstly because the thickness of aqueous lubricating film is small due to high bulk elasticity for hard materials according to soft EHL model ($h \propto E'^{-0.45}$). Additionally, hard engineering materials, especially those that are polished or cast, tend to display high surface roughness, and thus the formation of lubricating film becomes further hampered. A related problem is that despite the selection of low applied load, 2 N, to facilitate the formation of lubricating films, apparent contact pressure reaches *ca*. 16 MPa and 160 MPa for *h*-**HB** and *h*-**HL** (Table 2), respectively. Furthermore, as local asperity contact pressures of hard materials are much higher, plastic deformation and/or wear process are inevitably involved even in lubricated contacts. Judging from Tresca yield criterion [33], bulk plastic deformation is not likely to occur for any of the tribopairs in this study [34]. However,

plastic shear of the surface asperities is fairly probable for the two hard tribopairs, POM-POM and steel-glass. According to Greenwood and Williamson [35], for an exponential asperity distribution,

$$\Psi = \frac{E'}{H} \cdot \left( \frac{\sigma}{R_{asp}} \right)^{1/2} \quad (3)$$

where $E'$, σ, $H$ and $R_{asp}$ is the reduced Young's modulus, the roughness, the hardness and the average asperity radius of tribopair (for dissimilar material tribocontact, σ, $H$ and $R_{asp}$ of the softer material from the two materials in contact are used in the equation), a dimensionless plasticity index (ψ) can be introduced as a guideline for plastic shear of surface asperities; the contact will be elastic if ψ < ~0.69 and plastic (or fracture for brittle materials) if ψ > ~0.69. It is noted that ψ is independent of load. The ψ values of POM-POM and steel-glass pairs are 1.9 and 5.80, respectively, and, thus, plastic deformation of asperities for these hard pairs is expected. This is in accordance with wear tracks observed on POM, glass, and steel surfaces (data shown in Supplementary Data SD3). For POM-POM, the surface roughness along the sliding track was observed to decrease from *ca.* 223 nm to 133 nm ($R_q$) after MTM experiments (see Table 1). This could be attributed to lapping of the surfaces where the surface asperities deform plastically and thereby flattening the surface. On the other hand, for steel-glass pair, the surface roughness along the sliding track on glass increased from *ca.* 3 nm to 24 nm ($R_q$) after MTM experiments (see Table 1). This is also an indication of plastic deformation or fracture. In contrast, for all PDMS interfaces, ψ is much lower than 0.69 (Table 2) and no wear track was observed after the tribological contacts.

### 2.3.2. Soft Interfaces

Figure 5 shows *μ vs.* speed plots and *μ vs.* Sommerfeld number plots for *s*-**HB** interface (PDMS-PDMS) at various temperatures.

**Figure 5.** (**a**) *μ vs.* mean speed (**b**) *μ vs.* Sommerfeld number (mean speed × viscosity × load$^{-1}$) plots for *s*-**HB** interface (PDMS-PDMS) lubricated with water as characterized by MTM. All experiments were performed at 50% SRR. Temperature was increased from low (1 °C) to high (90 °C). Each point in the plots consists of averaging of three measurements. Error bars designate standard deviation

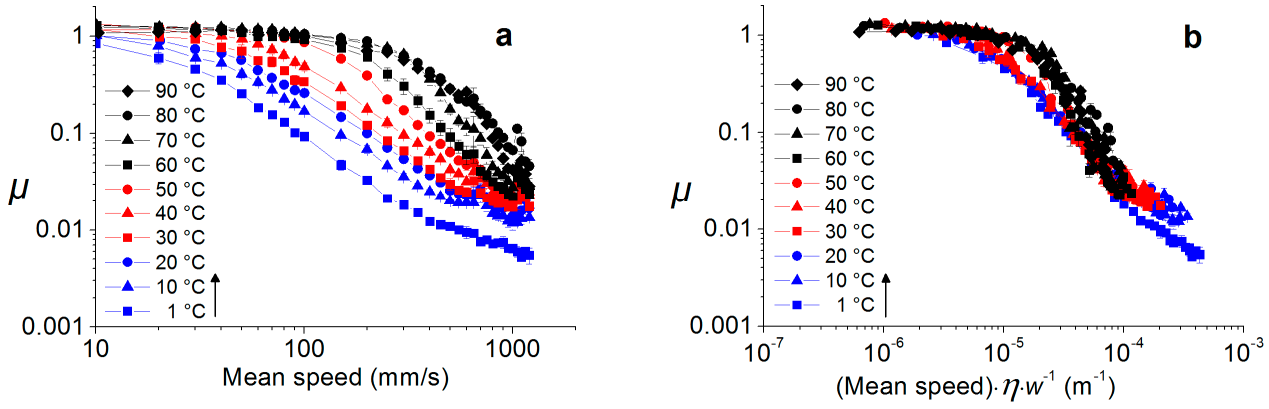

For this tribopair, large changes in $\mu$ values are observed as a function of speed at all temperatures, from $\mu$ being close to 1 down to 0.01. This trend is similar to that of *h*-**HL** interface (Figure 4), but effective lubricating properties in high-speed regime are not indebted from hydrophilicity of the interface, but from the softness of the tribopair. In fact, according to the theoretical prediction by soft-EHL model, where the bulk mechanical properties of the tribopair only is considered, *s*-**HB** interface is expected to form a large film thickness, for example as high as *ca.* 1 μm at 1000 mm/s, at room temperature (20 °C). As with *h*-**HL** interface, $\mu$ *vs*. Sommerfeld number plot (Figure 5b) shows a convergence of the data points on a master curve. $\mu$ *vs*. Sommerfeld number plots in Figure 5b suggest that the type of lubrication in high Sommerfeld number regime is mixed lubrication than full fluid-film lubrication judging from the lack of EHL transition in $\mu$.

Figure 6 shows $\mu$ *vs.* speed plots and $\mu$ *vs.* Sommerfeld number plots for *s*-**HL** interface (*ox*PDMS-*ox*PDMS), which is different only in surface hydrophilicity compared to *s*-**HB** interface, at various temperatures.

**Figure 6.** (**a**) $\mu$ *vs.* mean speed (**b**) $\mu$ *vs.* Sommerfeld number (mean speed × viscosity × load$^{-1}$) plots for *s*-**HL** interface (*ox*PDMS-*ox*PDMS) lubricated with water as characterized by MTM. All experiments were performed at 50% SRR. Temperature was increased from low (1 °C) to high (90 °C). Each point in the plots consists of averaging of three measurements. Error bars designate standard deviation.

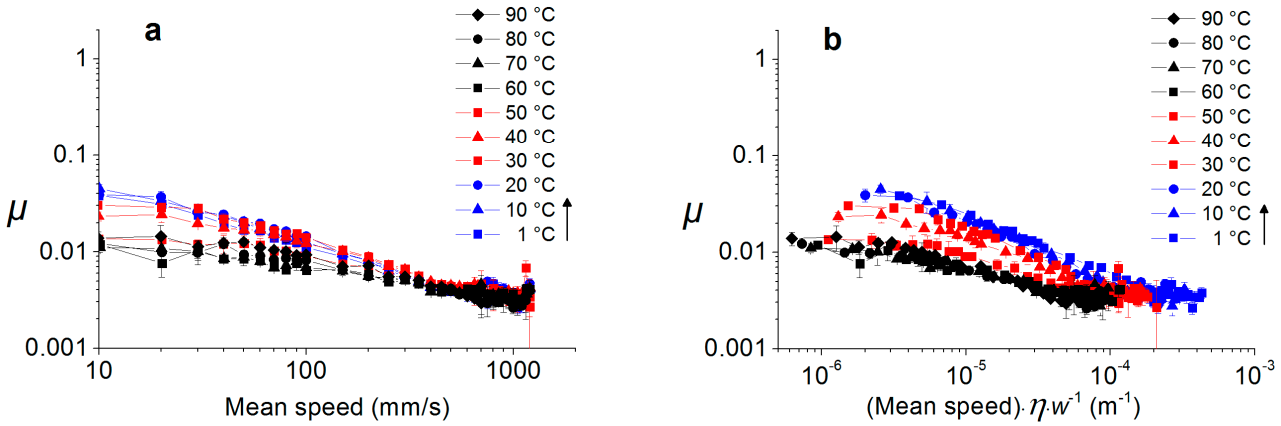


As a function of speed, a slight decrease of $\mu$ with increasing speed is also observed at all temperatures (Figure 6a). The data points over the universal line for the $\mu$ *vs.* Sommerfeld number plots (Figure 6b) appear to be somewhat scattered, however, the magnitude of scatter is very small, $\mu$ of ±0.02 (note that the Figure 6 is in log-log scale). Compared to *s*-**HB** interface, very low $\mu$ values, 0.01 or below, were reached from much lower Sommerfeld numbers. Highly enhanced lubricating properties of water for *s*-**HL** interface compared to *s*-**HB** interface were apparently due to higher hydrophilicity of *ox*PDMS surfaces.

Collectively, the influence of temperature on the lubrication with water was much more significant for soft contacts, apparently because of more feasible formation of lubricating films. When both bulk mechanical properties and surface roughness are considered, PDMS-PDMS contacts in this study are expected to provide λ parameters that are higher than 4 in the high-speed regime (1000 mm/s) at all temperatures (Figure 2c). Nevertheless, no transition to increasing trend in $\mu$ values in the highest

Sommerfeld number was observed, even for *s*-**HL** interface where surface wetting and entrainment of water into the contact area is substantially facilitated. This may suggest that λ parameters within the temperature range of 1 to 90 °C, *i.e.*, *ca.* 12 to 4, are still not sufficient to activate fluid-film lubrication. Previous studies of aqueous lubrication of soft contacts involving PDMS showed clear transition of $\mu$ to increasing trend with increasing speed in high-speed regime [29,36–38]. However, the base fluids in those studies were mixtures of water and corn syrup [36,37] or glycerol [38], and the viscosities of the fluids were a few orders of magnitude higher than that of water. Even with fluids with much higher viscosity, the transition to fluid-film lubrication was reported to occur from λ is *ca.* 10 [29]. With neat water, it appears that characteristic transition to increasing trend of $\mu$ for EHL is not feasible under the experimental conditions in this study. In turn, this is resulting from that distilled water is a representative Newtonian fluid and the increase of friction shear forces due to viscous shear is too small to be detected by MTM (discussed in detail in SD4, Supplementary Data).

### *2.4. Temperature Dependence of Water-Lubricated Tribocontacts*

As an overview for the influence of temperature on the lubricating properties of water, the plots for $\mu$ values obtained from the four tribopairs, (a) *h*-**HB**; (b) *h*-**HL**; (c) *s*-**HB**, and (d) *s*-**HL**, are displayed as a function of temperature in Figure 7. In this plot, the $\mu$ values at 10, 100 and 1000 mm/s are presented.

**Figure 7.** $\mu$ *vs.* temperature plots for (**a**) *h*-**HB** (POM-POM); (**b**) *h*-**HL** (steel-glass); (**c**) *s*-**HB** (PDMS-PDMS); (**d**) *s*-**HL** (*ox*PDMS-*ox*PDMS) interfaces lubricated with water. All experiments were performed at 50% SRR.

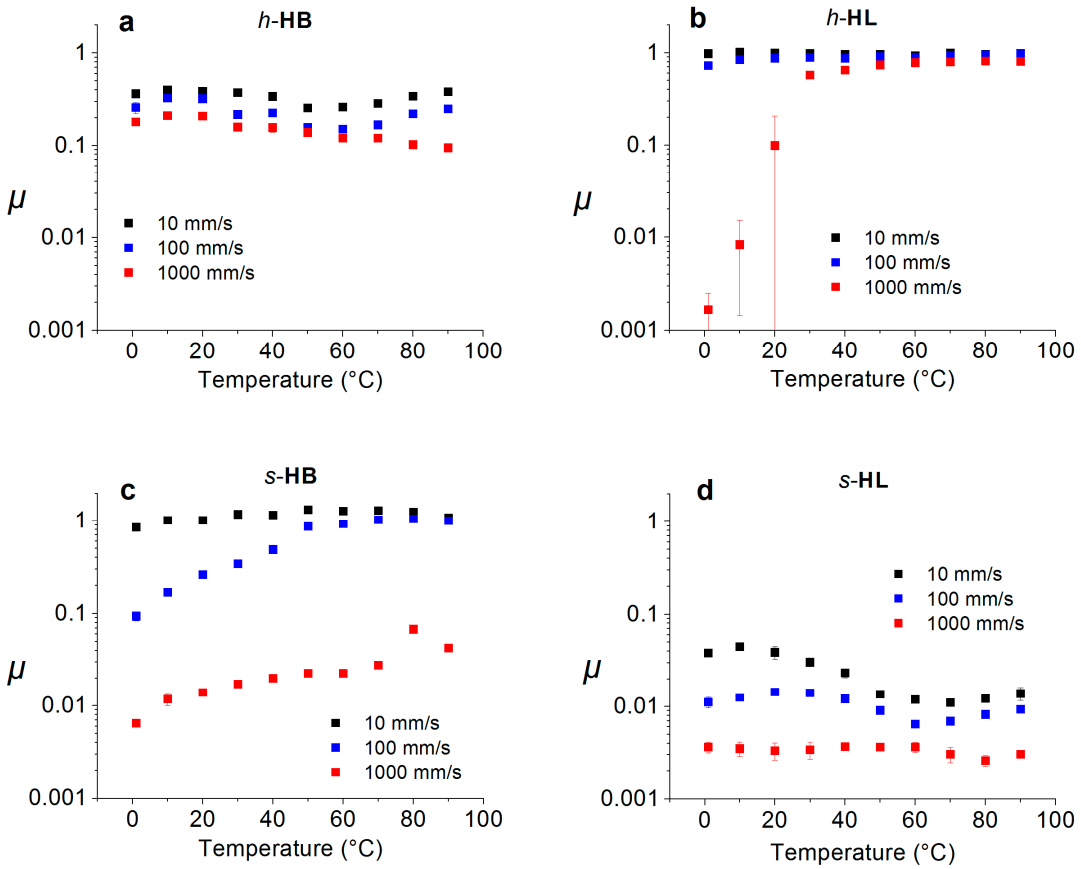

Figure 7 clearly shows that the influence of temperature on the lubricating properties of water is different for different tribopairs. For *h*-**HB** interface, nearly ignorable temperature dependence of $\mu$ is observed at all temperatures, due to hydrophobic, rough, as well as hard characteristics of the interface. For both *h*-**HL** and *s*-**HB** interfaces, a gradual increase of $\mu$ with increasing temperature is visible in high-speed regimes, due to the gradually decreasing viscosity of water with increasing temperature; however, this trend is much clearer for *s*-**HB** interface, and generally much lower $\mu$ values are observed from this interface. Even though a generalization is not possible at this stage, this observation suggests that mechanical properties of the tribopair may be more important than surface hydrophilicity in determination of the efficacy of lubrication with water. Lastly, for *s*-**HL** interface, weak temperature dependence of the lubricating properties is also observed. However, the $\mu$ values are maintained low at all conditions, suggesting that sufficient lubricating films might be sustained despite the changes in speed and temperature. Nevertheless, even at the highest speed (1200 mm/s), dominant lubricating mechanism for this interface appears to be boundary or mixed lubrication, judging from the lack of changes in $\mu$ values with increasing temperature. If a full-fluid film is formed between the two rubbing surfaces and the applied loads are entirely taken up by the fluid, decrease of fluid viscosity should lead to decreased friction as a result of reduced viscous drag. The lack of increasing trend of $\mu$ with increasing speed (Figure 5) and the lack of decrease in $\mu$ with increasing temperature (Figure 6d) collectively suggest that the full-fluid lubrication is still not achieved in this condition. Alternatively, the magnitude of change in $\mu$ from the formed fluid film is too small to be detected by MTM (SD4 in Supplementary Information).

## 3. Experimental Section

### *3.1. Tribopairs*

Four different tribopairs have been employed (ball-disc): (a) polyoxymethylene-polyoxymethylene (POM-POM) to represent *h*-**HB** interface; (b) steel-glass to represent *h*-**HL** interface; (c) poly(dimethylsiloxane)-poly(dimethylsiloxane) (PDMS-PDMS) to represent *s*-**HB** interface; (d) oxidized poly(dimethylsiloxane)-oxidized poly(dimethylsiloxane) (*ox*PDMS-*ox*PDMS) to represent *s*-**HL** interface. POM discs were prepared by cutting from commercially available rods (Rias A/S, Roskilde, Denmark). Commercially available POM balls (¾ inch (19.05 mm) in diameter) were used as received (Precision Plastic Ball Company, Franklin Park, IL, USA). Commercially available bearing steel balls (AISI 52100) and glass discs were employed (PCS Instruments, London, UK). PDMS balls and discs were fabricated from a two-component kit (SYLGARD® 184, Dow Corning, Midland, MI, USA) consisting of base PDMS and crosslinker. The PDMS base and crosslinker were mixed at 10:1 wt. ratio, and dispersed air bubbles formed during mixing were removed by a vacuum using an oil pump. For PDMS disc, the mixture fluid was poured on top of the steel disc in a plastic mold with nearly same diameter and cured overnight at 70 °C. PDMS-coated disc was obtained by removing the mold. The thickness of PDMS disc on top of the steel disc was 2 mm. PDMS balls with ¾ inch (19.05 mm) in diameter were cast in a home-machined aluminum mold.

Surface roughness of the discs and balls was characterized by acquiring root-mean-square roughness ($R_q$) from topographic images over a 100 μm × 100 μm area with tapping-mode AFM.

Three different spots were characterized for statistical evaluation. In order to obtain the average asperity radius of the tribopairs, surface topographic images of 1 μm × 1 μm area were obtained. The full list of the surface roughness and asperity radii of the tribopairs is shown in Table 1. Bruker AFM model Dimension® Edge™ and NanoScope 8.02 software were used for AFM imaging, with NanoScope Analysis software (ver. 1.40) for calculating roughness and asperity radii.

**Table 1.** Bulk mechanical and surface properties of the tribopair materials.

| Substrate | Young's Modulus (MPa) | Poisson's Ratio | Hardness (MPa) | Roughness, $R_q$, (nm) | | Asperity Diameter Average (nm) | | Static Water Contact Angle (°) |
|---|---|---|---|---|---|---|---|---|
| | | | | Disc | Ball | Disc | Ball | |
| PDMS | 2.0 [39] (7.0) [a,40] | 0.5 [39] | 2.2 [f] | 1.6 ± 0.3<br>2.9 ± 0.7<br>(plasma tr.) | HB:<br>121.4 ± 36.4<br>HL:<br>116.9 ± 50.6 | No asperities | HB: 1448 ± 300<br>HL: 2189 ± 246 | pristine:<br>105.6 ± 2.2 [e]<br>plasma tr.:<br><2 |
| POM | 3,100 [41] | 0.35 [41] | 354 [41],[h] | 223 ± 51<br>Wear track:<br>133 ± 44 | 659 ± 179<br>414 ± 180 | 5086 ± 504 | 4743 ± 1419 | pristine:<br>84.8 ± 2.9 [c] |
| Steel (AISI E 52100) | 210,000 [41] | 0.3 [41] | 8,319 [41] | - | 26.1 ± 5.5<br>Wear track: | | 116 ± 17 | pristine:<br>57.5 ± 0.7 [b]<br>plasma tr.:<br><2 |
| Glass | 73,000 [42] | 0.17 [42] | 7,848 [41] | 2.9 ± 0.3<br>Wear track: | - | 73 ± 49 | | pristine:<br>32.9 ± 3.3<br>plasma tr.:<br><2 |

[a] 7.0 MPa represents the effective Young's modulus of a 2 mm PDMS layer on steel; [b] Contact angle of water on 304 steel plate; [c] Hydrophobic surfaces with high roughness can have increased contact angle due to Wenzel effect; [e] PDMS disc (smooth); [f] Estimated from the (tensile strength)/3.45. 7.5 MPa/3.45 = 2.2 MPa [42,43]; [h] Estimated from Rockwell M hardness.

### *3.2. Hydrophilization of Substrates*

The static water contact angles on POM and PDMS surfaces were 84.8 ± 2.9° and 105.6 ± 2.2°, respectively. In order to hydrophilize balls and discs, including PDMS, steel, and glass, a plasma cleaner/sterilizer (Harrick Plasma, model PDC-002, New York, NY, USA) was employed. Air plasma treatment for 3 min lowered the water contact angles of the substrates significantly. For *ox*PDMS and glass, the contact angles were less than 2°. See Table 1 for contact angle values of pristine and hydrophilized substrates.

### *3.3. Lubricant*

Millipore water (resistivity higher than 18 MΩ·cm) was employed as lubricant, if not stated otherwise. The viscosity of water within the temperature range from 0 ºC to 100 ºC is shown in Table 3 [17].

### *3.4. MTM (Mini-Traction Machine)*

A mini-traction machine (MTM) (MTM2, PCS Instruments, London, UK) with software version 3.2.3.0 was employed to investigate the frictional properties of tribopairs lubricated with water. The principal setup of MTM consists of independently rotating ball and disc immersed in fluid lubricant with the possibility to control load and temperature. The friction forces are measured with a strain gauge connected to ball shaft arm. Coefficient of friction, $\mu$, is defined from the relationship, $\mu = F_{friction}/F_{load}$. Independent control of disc and ball speeds allows for the variation of the degree of slide/roll ratio. The mean speed is defined as $[|speed_{ball} - speed_{disc}|/2]$. The slide/roll ratio, SRR (%), is defined as $SRR(\%) = (|speed_{ball} - speed_{disc}|)/[(speed_{ball} + speed_{disc})/2] \times 100\%$, where 0% SRR represents pure rolling and 200% SRR represents pure sliding. The SRR in this study was 50% unless otherwise stated. A pair of measurements is performed to yield a mean $\mu$ at each mean speed; in one measurement, the speed of disc is higher and in the other one, the speed of ball is higher. The mean speed was changed from 10 mm/s to 1200 mm/s for all cases. The data points in Figures 2–5 are average values of three measurements, and the error bars represent the standard deviation. The applied load was 2 N for hard contacts (POM-POM and steel-glass) and 5 N soft contacts (PDMS-PDMS and *ox*PDMS-*ox*PDMS), respectively. Apparent contact pressures for each tribopair are shown in Table 2.

**Table 2.** Contact characteristics of the tribopairs: load, Hertzian contact pressure, reduced Young's modulus ($E'$), mean surface roughness ($\sigma^*$), and plasticity index: $\psi = (E'/H)\cdot(\sigma/R_{asp})^{1/2}$.

| | **Hydrophobic** | **Hydrophilic** |
|---|---|---|
| **Soft** | **PDMS †-PDMS †** | **PDMS-PDMS** |
| Load | 5 N | 5 N |
| $E'$ | 2.07 | 2.07 |
| Pressure | 0.24 MPa | 0.24 MPa |
| $\sigma^*$ | 121.4 nm | 116.9 nm |
| $\psi$ | 0.22 | 0.27 |
| **Hard** | **Steel †-glass †** | **POM-POM** |
| Load | 2 N | 2 N |
| $E'$ | 56,700 MPa | 1766 MPa |
| Pressure | 160 MPa | 16 MPa |
| $\sigma^*$ | 26.3 nm | 695 nm |
| $\psi$ | 5.8 | 1.9 |

† Plasma-treated.

Since MTM operates with an enclosed pot inside which a lubricated tribocontact is formed, it is feasible to control the temperature. Higher temperatures than ambient were obtained by heating the pot with a built-in thermistor, whereas lower temperatures than ambient were obtained by circulating a coolant surrounding the pot. The lowest temperature at which the friction measurements were conducted was 1 °C. From 10 °C to 90 °C, the coefficients of friction were measured at 10 °C increments. The temperature was automatically regulated by the MTM control units with an accuracy of ±1 °C, with thermocouple inside the pot. The order of measurements was from the lowest to highest

temperature, where three consecutive measurements series at each temperature were performed to give a statistical average.

**Table 3.** Viscosity of water as a function of temperature [17] (* = estimated value).

| ***T*, Temperature** | ***η*, Viscosity** |
|---|---|
| (°C) | (mPa·s) |
| 0 | 1.793 |
| 1 * | 1.750 * |
| 10 | 1.307 |
| 20 | 1.002 |
| 30 | 0.798 |
| 40 | 0.653 |
| 50 | 0.547 |
| 60 | 0.467 |
| 70 | 0.404 |
| 80 | 0.354 |
| 90 | 0.315 |
| 100 | 0.282 |

## 4. Conclusions

In this study, the influence of temperature on the lubrication properties of water has been explored by employing tribopairs with distinctively different mechanical properties and surface hydrophilicity, namely *h*-**HB** (POM-POM), *h*-**HL** (steel-glass), *s*-**HB** (PDMS-PDMS), and *s*-**HL** (*ox*PDMS-*ox*PDMS) interfaces. The temperature was varied from 1 to 90 °C. The theoretically predicted lubricating film thicknesses, and in turn, λ parameter estimates by further taking the surface roughness into account, were compared with the coefficients of friction obtained by MTM experiments. It was shown that soft EHL model considering mechanical properties of the tribopair only was not sufficiently accurate to predict the feasibility of fluid film formation. While λ parameters were estimated as high as *ca*. 12 for *s*-**HL** interface at an optimum condition, no clear indication of transition to fluid-film lubrication was observed or the change in the coefficient of friction was too small to be detected by MTM. For hard tribopairs, *h*-**HB** (POM-POM) and *h*-**HL** (steel-glass) interfaces, the influence of temperature on the frictional properties was weak due to high elasticity moduli and high surface roughness, and consequently hampered formation of aqueous lubricating films. *h*-**HL** interface (steel-glass) displayed some degree of lubricity at the highest entrainment speeds and low temperatures due to surface hydrophilicity. For soft contacts, the influence of temperature on the frictional properties was more apparent and drastic, reflecting the feasible formation of aqueous lubricating films. However, the lack of characteristic transition to increasing $\mu$ trend, even for *s*-**HL** interface (*ox*PDMS-*ox*PDMS) in the highest speed regime, together with the lack of changes in $\mu$ with increasing temperature (decreasing viscosity) at the highest speed, implies that the soft EHL films were not generated with neat water as sole lubricant. Alternatively, the magnitude of $\mu$ change in this condition may be too small to be sensed by MTM. Establishment of the influence of temperature on the tribocontacts lubricated with water in this study is expected to provide a useful reference in understanding the respective role of

base fluid (water) and additives for more complex aqueous lubricants under the variation of temperature for a variety of tribopairs.

**Acknowledgments**

The authors acknowledge the financial supports from the Danish Council for Independent Research (DFF), Technology and Production Sciences (FTP) (10-082707) and European Research Council (ERC) (Funding Scheme: ERC Starting Grant, 2010, Project Number 261152) for this study.

**Author Contributions**

Troels Røn is the first author of this article, and his contribution includes the design of experiments, performing experiments, interpretation of the collected data, and writing the manuscript. Seunghwan Lee is the principal investigator for this research, and his contribution includes the plan of the study, design of experiments, interpretation of the collected data, and revision of the manuscript.

**Conflicts of Interest**

The authors declare no conflict of interest.

**References and Notes**

1. Dedinaite, A.; Pettersson, T.; Mohanty, B.; Claesson, P.M. Lubrication by organized soft matter. *Soft Matter* **2010**, *6*, 520–1526.
2. Dai, Z.; Tong, J.; Ren, L. Researches and developments of biomimetics in tribology. *Chin. Sci. Bull.* **2006**, *51*, 2681–2689.
3. Ahlroos, T.; Hakala, T.J.; Helle, A.; Linder, M.B.; Holmberg, K.; Mahlberg, R.; Laaksonen, P.; Varjus, S. Biomimetic approach to water lubrication with biomolecular additives. *Proc. IMechE. Part J* **2011**, *225*, 1013–1022.
4. Lee, S.; Spencer, N.D. Achieving ultra-low friction by aqueous, brush-assisted lubrication. In *Superlubricity*; Erdemir, A., Martin, J.-M., Eds.; Elsevier: Amsterdam, The Netherlands, 2007; pp. 365–396.
5. Klein, J. Hydration lubrication. *Friction* **2013**, *1*, 1–23.
6. Neville, A.; Morina, A.; Liskiewicz, T.; Yan, Y. Synovial joint lubrication—Does nature teach more effective engineering lubrication strategies? *Proc. IMechE Part C* **2007**, *221*, 1223–1230.
7. Crockett, R. Tribology of natural articular joints. In *Aqueous Lubrication: Natural and Biomimetic Approaches*; Spencer, N.D., Ed.; Elsevier: World Scientific, IISc Press: Singapore, 2014; pp. 1–32.
8. Wang, B.; Sun, J.; Wu, Y. Lubricating performances of nano organic-molybdenum as additives in water-based liquid during cold rolling. *Adv. Mater. Res.* **2011**, *337*, 550–555.
9. Wang, Z.; Gao, D. Comparative investigation on the tribological behavior of reinforced plastic composite under natural seawater lubrication. *Mater. Design* **2013**, *51*, 983–988.

10. Lee, S.; Müller, M.; Vörös, J.; Pasche, S.; de Paul, S.; Textor, M.; Ratoi, M.; Spikes, H.A.; Spencer, N.D. Boundary lubrication of oxide surfaces by poly(L-lysine)-*g*-poly(ethylene glycol) (PLL-*g*-PEG) in aqueous media. *Tribol. Lett.* **2003**, *15*, 231–239.
11. Ratoi, M.; Spikes, H.A. Lubricating properties of aqueous surfactant solutions. *Tribol. Trans*. **1999**, *42*, 479–486.
12. Chinas-Castillo, F.; Lara-Romero, J.; Alonso-Nunez, G.; Lopez-Velazquez, A. Tribology of aqueous thiomolybdate and thiotungstate additives in low-pressure contacts. *Tribol. Trans*. **2013**, *56*, 366–373.
13. Penga, Y.; Hua, Y.; Wang, H. Tribological behaviors of surfactant-functionalized carbon nanotubes as lubricant additive in water. *Tribol. Lett*. **2007**, *25*, 247–253.
14. Mens, J.W.M.; de Gee, A.W. Friction and wear behavior of 18 polymers in contact with steel in environments of air and water. *Wear* **1991**, *149*, 255–268.
15. Hsu, J.-P.; Lin, S.-H. Temperature dependence of the viscosity of nonpolymeric liquids. *J. Chem. Phys.* **2003**, *118*, 172–178.
16. Bair, S.; Jarzynski, J.; Winer, W.O. The temperature, pressure and time dependence of lubricant viscosity. *Tribol. Int.* **2001**, *34*, 461–468.
17. CRC. *Handbook of Chemistry and Physics*, 89th ed.; Taylor and Francis Group LLC: Boca Raton, FL, USA, 2009.
18. Tripaldi, G.; Vettor, A.; Spikes, H.A. Friction behavior of ZDDP films in the mixed, boundary/EHD regime. *SAE Trans*. **1996**, *105*, 1819–1830.
19. Dardin, A.; Hedrich, K.; Müller, M.; Ksenija, T.-M.; Spikes, H.A. Influence of Polyalkylmethacrylate Viscosity Index Improvers on the Efficiency of Lubricants. *SAE Tech. Paper* **2003**, doi:10.4271/2003-01-1967.
20. Hamrock, B.J.; Dowson, D. Minimum film thickness in elliptical contacts for different regimes of fluid-film lubrication. In Proceedings of the 5th Leeds-Lyon symposium on tribology. Mechanical Engineering Publication: Bury St Edmunds, Suffolk, UK, 1979; pp. 22–27.
21. Esfahanian, M.; Hamrock, B.J. Fluid-film lubrication regimes revisited. *Tribol. Trans*. **1991**, *34*, 628–632.
22. Lee, S.; Spencer, N.D. Aqueous lubrication of polymers: Influence of surface modification. *Tribol. Int.* **2005**, *38*, 922–930.
23. Kumikov, V.K.; Khokonov, K.B. On the measurement of surface free energy and surface tension of solid metals. *J. Appl. Phys*. **1983**, *54*, 1346–1350.
24. Wu, S. Surface and interfacial tensions of polymer melts II. *J. Phys. Chem*. **1970**, *74*, 632–638.
25. Lui, M.; Sun, J.; Chen, Q. Influences of heating temperature on mechanical properties of polydimethylsiloxane. *Sens. Actuators A* **2009**, *151*, 42–45.
26. Hutchings, I.M. *Tribology: Friction and Wear of Engineering Materials*; Elsevier: London, UK, 1992.
27. Stachowiak, G.; Batchelor, A.W. *Engineering Tribology*, 3rd ed.; Butterworth-Heinemann: Burlington, MA, USA, 2005.
28. Cassin, G.; Heinrich, E.; Spikes, H.A. The influence of surface roughness on the lubrication properties of adsorbing and non-adsorbing biopolymers. *Tribol. Lett*. **2001**, *11*, 95–102.

29. Bongaerts, J.H.H.; Fourtouni, K.; Stokes, J.R. Soft-tribology: Lubrication in a compliant PDMS–PDMS contact. *Tribol. Int.* **2007**, *40*, 1531–1542.
30. Glovnea, R.P.; Forrest, A.K.; Olver, A.V.; Spikes, H.A. Measurement of sub-nanometer lubricant films using ultra-thin film interferometry. *Tribol. Lett*. **2003**, *15*, 217–230.
31. Guo, F.; Wong, P.L.; Fu, Z.; Ma, C. Interferometry measurement of lubricating films in slider-on-disc contacts. *Tribol. Lett*. **2010**, *39*, 71–79.
32. Bongaerts, J.H.H.; Day, J.P.R.; Marriott, C.; Pudney, P.D.A.; Willamson, A.M. *In situ* confocal Raman spectroscopy of lubricants in a soft elastohydrodynamic tribological contact. *J. App. Phys*. **2008**, *104*, doi:10.1063/1.2952054.
33. Gohar, R.; Rahnejat, H. *Fundamentals of Tribology*; Imperial College Press: London, UK, 2012.
34. Onset of plastic bulk deformation due to shear stress under normal load can be judged by Tresca yield criterion (sphere on plane with ideal smoothness), $\frac{3}{2}(p_m)_Y = 1.60\,Y \approx 0.6H \Rightarrow (p_m)_Y \approx 0.4H$, where $p_m$ is the mean pressure, $Y$ is the elastic limit and $H$ is the hardness of the softer of the two materials in contact. The thresholds for PDMS-PDMS, POM-POM, and steel-glass are 0.8, 142 and 3140 MPa, respectively, that the contact pressures in this study are sufficiently lower than these thresholds.
35. Greenwood, J.A.; Williamson, J.B.P. Contact of nominally flat surfaces. *Proc. R. Soc. Lond. Ser. A* **1966**, *295*, 300–319.
36. De Vicente, J.; Stokes, J.R.; Spikes, H.A. The frictional properties of Newtonian fluids in rolling-sliding soft-EHL contact. *Tribol. Lett*. **2005**, *20*, 273–286.
37. De Vicente, J.; Stokes, J.R.; Spikes, H.A. Soft lubrication of model hydrocolloids. *Food Hydrocoll.* **2006**, *20*, 483–491.
38. Nalam, P.C.; Clasohm, J.N.; Mashaghi, A.; Spencer, N.D. Macrotribological studies of Poly(L-lysine)-*graft*-poly(ethylene glycol) in aqueous glycerol mixtures. *Tribol. Lett*. **2010**, *37*, 541–552.
39. Mark, J.E. *Polymer Data Handbook*; Oxford University Press, Inc.: New York, NY, USA, 1999.
40. The effective Young's modulus of composite layers in the antiparallel direction of the layers is calculated from the relation: $E = (f_1/E_1 + f_2/E_2)^{-1}$, where $f_x$ is volume fraction the material and $E_x$ is the bulk Young's modulus. For the case of 2 mm PDMS layer on a 5 mm thick steel disc the effective Young's modulus is: $((0.2/0.7)/2\text{ MPa} + (0.5/0.7)/207\text{ GPa})^{-1} = 7.0$ MPa.
41. MatWeb Homepage. Available online: http://www.matweb.com (accessed on 1 May 2014).
42. Callister, W.D.J. *Material Science and Engineering, an Introduction*, 7th ed.; John Wiley & Sons, Inc.: New York, NY, USA, 2007.
43. Mata, A.; Fleischman, A.J.; Roy, S. Characterization of polydimethylsiloxane (PDMS) properties for biomedical micro/nanosystems. *Biomed. Microdev*. **2005**, *7*, 281–293.